Design of P-Type Photovoltaic Cells Resistant to Potential-Induced Degradation

Josef Hylský, Dávid Strachala, Jiří Hladík, Pavel Čudek, Tomáš Kazda, Jiří Vaněk, Petr Vyroubal, and Jiří Starý

***Abstract*—The manufacturing process and the new structure of the potential-induced degradation (PID) resistive photovoltaic (PV) cells are described. PV cells are produced in the commonly used technological steps. The structure is modified by using the phosphorus silicate glass (PSG) layers after the diffusion process when the PV cell emitter is created. This modification is made directly at one of the produced sets in the serial production of 6-in PV cells. In the newly created PV cells, the basic parameters (fill factor, V_{OC}, I_{SC}, and P_{MAX}) and the thickness of the PSG layer were measured. The values of the parameters were compared with those of the reference PV cells without the PSG layer. The results show that the effect of the PSG layer on the PV cell efficiency is negligible. Both groups of PV cells (the reference group and the new structures) were potential-induced degraded. The PV cells with the PSG layer have shown properties resistive against PID.**

***Index Terms*—Phosphorus silicate glass (PSG) layer, photovoltaic (PV) cell, potential-induced degradation (PID), potential-induced degraded resistive structure.**

I. Introduction

RENEWABLE sources of electricity are currently widely discussed not only in specialized scientific centers, but in public as well. One of main renewable energy sources is photovoltaic (PV), where direct solar radiation is converted into electricity. PV is a widespread alternative power source installed on family houses or over large areas with the powerful PV systems. For the generation of high power, the PV modules are connected in series in the so-called strings. When a large number of PV modules are connected in series, a negative voltage potential occurs between the grounded aluminum frame of the PV module and PV cells in the negative pole of the string. The negative voltage potential may cause degradation known as potential-induced degradation (PID). PID may result in a significant reduction in the total PV power plant output (≈30%) [1]. Any reduction in the power output of the PV system has a negative impact on its efficiency, which is reflected in the overall system return rate. For these reasons, it is necessary to eliminate the degradation as soon as possible, or, better yet, prevent it.

The origin of PID and its effect on the PV cells is currently discussed within the scientific community around the world. A very good description of the degradation of classical p-type PV cells with a silicon-based front emitter was given by the Fraunhofer Center for Silicon Photovoltaics (FCSP) [2]–[7]. The FCSP has described the movement of the sodium ions from the cover glass through the PV module structure up to the silicon oxide layer, SiO_2, in the PV cells. According to the publications, sodium ions diffuse into the silicon stacking faults due to the high voltage potential and cause short circuits of the PV cell p-n junction. The described explanation at the atomic level is supplemented by a publication describing a possible reversible process, where the influence of the reversed electric field and temperature causes the separation of sodium ions from the stacking faults. In this case, the short circuits will be reduced [8].

This type of PID was called a PID-shunt (shortly PID-s) because of p-n junction short circuits [9]. PID of n-type PV cells with a front emitter was described in [10]. Other types of n-type PV cells such as interdigitated back-contact cells are described in [11] and [12]. In these types of cells, the output power is reduced due to an increased surface recombination velocity caused by a positive voltage potential. On the other hand, in [12], Swanson describes the influence of a negative voltage potential. In [11], Naumann *et al.* introduced the so-called PID-p degradation due to polarization. The influence of PID on the n-type PV cells with a rear-side emitter is described in [13]. Also described in [13] is the dependence of PID on the reduction of PV cell parameters such as the current density J_{SC} and the open-circuit voltage V_{OC} due to increased surface recombination of minor charge carriers.

The above-mentioned publications point out various PID influences, but all of them come to the same conclusion. The high voltage potential between the module frame and the PV cells allows the sodium ion pass through the PV module structure to the PV cells.

The PID elimination can be considered at three levels: at the PV system level, at the PV module level, and in the PV cells [1]. At the PV power plant level, PID can be eliminated by PID regenerators known as PID doctors [19]. These regenerative systems are installed in string inverters. When the PV power plant does not generate electrical energy, this system connects to the PV module and the frame. The PID doctors apply reverse

Manuscript received March 27, 2018; revised May 2, 2018; accepted May 17, 2018. This research was carried out at the Centre for Research and Utilization of Renewable Energy. This work was supported by the Ministry of Education, Youth and Sports of the Czech Republic under NPU I program under Project LO1210. *(Corresponding author: Josef Hylský.)*

J. Hylský, D. Strachala, P. Čudek, T. Kazda, J. Vaněk, P. Vyroubal, and J. Starý are with the Department of Electrical and Electronic Technology, Brno University of Technology, 616 00 Brno, Czech Republic (e-mail: xhylsk00@stud.feec.vutbr.cz; xstrac07@stud.feec.vutbr.cz; cudekp@feec.vutbr.cz; kazda@feec.vutbr.cz; vanekji@feec.vutbr.cz; vyroubal@feec.vutbr.cz; stary@feec.vutbr.cz).

J. Hladík is with Fill Factory s.r.o., 756 61 Rožnov pod Radhoštěm, Czech Republic (e-mail: jiri.hladik@fillfactory.cz).

Color versions of one or more of the figures in this paper are available online at http://ieeexplore.ieee.org.

Digital Object Identifier 10.1109/JPHOTOV.2018.2841188

polarity opposite to the polarity during power generating. Inverted electric field removes the sodium ions embedded in the stacking faults, where they have been stacked during daylight. As a result, the p-n junction short circuits will disappear. As shown in [14], regenerated PV cells with reversed voltages achieve power output near the state before PID degradation (80–96%). However, additional investment in the PV power is required. In addition, the high purchase price of the PID doctors needs to be taken into account.

The PV module level (standard type as well as glass to glass) deals with the protection against PID by selecting the material used in the sandwich structure of the PV module. For example, it has been proven in [15] that lamination materials used for protection and galvanic separation of PV components can directly affect the extent of the PID degradation. PID can be rapidly slowed down by replacing the widely used ethylene vinyl acetate (EVA) material with an alternative material with slower sodium ion migration. The alternative materials can be partially neutralized by ethylene methacrylic acid copolymer and EVA copolymer [15] or polyolefin elastomer [16]. In [17]–[19], the PID is accelerated by environmental influences such as humidity and temperatures, and therefore, proper encapsulation plays a major role in the PID susceptibility of the PV module.

The third level where PID can be avoided is the PV cell. This level focuses on modifying the PV cell structure during the manufacturing process. The manufacturing of two- and three-layer antireflection coatings to reduce the susceptibility to PID is described in [20]. The disadvantage of this modification may be in the PV cell efficiency reduction due to the refractive index of the new layers. The PID susceptibility of p-type bulk PV cells is largely influenced by an emitter sheet resistance parameter, more precisely the concentration of phosphorus in the n-type emitter. Extremely high phosphorus concentrations on the surface of the emitter can prevent the p-n junction contamination by the sodium ion [21].

PID generally reduces the performance of the PV cells, PV modules, or entire PV systems, which leads to a prolonged return on investment. Protection against PID by the PID doctors or by an alternative material requires increased financial costs. It is, therefore, desirable to focus on methods for eliminating PID with the lowest possible cost of the manufacturing process, the same manufacturing steps, and PV cell efficiency without major changes. Therefore, this publication focuses on modifying the structure of a PV cell that meets the criteria described above.

During the serial production of standard 6-in p-type PV cells, the structure was modified in a half of one batch. The parameters of the reference and newly created PV cells are compared in order to determine the effect of the modified structure to PID resistivity. There is an emphasis on minimal interference with the current technological steps of the PV cell production process.

II. Sample Preparation

To prevent the entry of sodium ions into the structure of the PV cell, a layer of phosphorus silicate glass (PSG) was used. This layer is created during the solar cell emitter diffusion process. The conventional diffusion process consists of two steps: the prediffusion step and the drive-in step. In our case, the diffusion process was adapted to the production of the n^+ emitter on the p-type substrate.

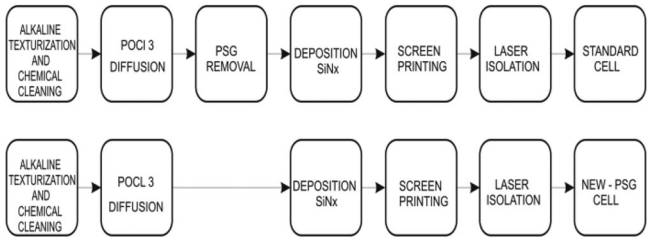

Fig. 1. Individual technological steps for the manufacturing of the PV cells. (First line) Reference samples. (Second line) New PV cell samples with the PSG layer.

In the first step, a layer containing SiO_2 and P_2O_5 is formed on the surface by the decomposition of $POCl_3$

$$4POCl_3 + 3O_2 \rightarrow 2P_2O_5 + 6Cl_2. \quad (1)$$

This way, a layer of PSG is produced, which is a source of phosphorus for the n-type concentration profile. The PSG dissociation into phosphorus and silicon dioxide is followed by the diffusion of phosphorus into the silicon substrate volume

$$2P_2O_5 + 5Si \rightarrow 4P + 5SiO_2. \quad (2)$$

The PSG layer is normally removed in a solution of hydrofluoric acid after the emitter and p-n junction formation. This layer is not removed in our samples because of discovered PID resistive properties.

Fig. 1 illustrates the steps of producing new and reference PV cells. For the texture of the surface, alkaline etching in sodium hydroxide was used.

Under common diffusion conditions, the thickness of the PSG layer is given by the parabolic function depending on temperature, time, and gas flow. The diffusion parameters affect the concentration of phosphorus in the PSG layer and in the PSG/silicon interface, where electrically inactive phosphorus precipitates can increase the surface recombination of minor carriers in the PV cell emitter region. The concentration of electrically inactive phosphorus at the PSG/Si interface can be reduced by proper parameter setting (especially $POCl_3$–N_2 gas flow), which eliminates the emitter sheet resistance increase [23].

The manufactured 6-in PV cells were first cut by laser and then broken into small samples (2×2 cm^2). This procedure prevents short circuit of the p-n junction at the PV cell edges. The samples were contacted, and subsequently, PV "minimodules" were created. A standard 0.45-mm EVA foil was used as the encapsulating material. PV cells with the EVA foil were laminated between 2.8-mm-thick glasses. A copper electrode source was attached to the front of the minimodule and then connected to the positive pole of the dc source. The negative pole of the dc source was connected to the contacts of PV cells. Such a connection created an electric field causing PID. Conductive adhesion between the glass and the electrode was enhanced by inserting a conductive layer, as shown in Fig. 2.

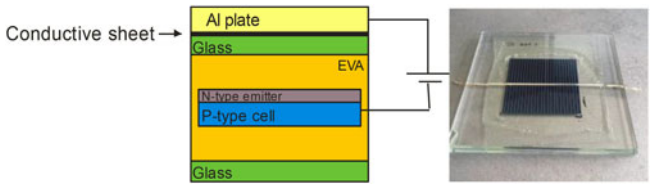

Fig. 2. Structure of the PV module sample with an electrode attached to the positive pole of the dc source and a real photo of the sample prepared for the PID.

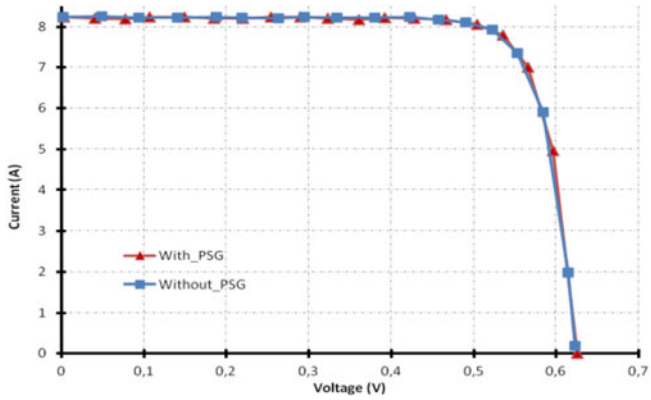

Fig. 3. *I–V* characteristics of the newly created sample (with the PSG layer) and the reference sample (without the PSG layer).

Workplace for degradation consisted of the Stericell 55 climate chamber, the high-voltage source IM6-re, and the *I–V* Curve Tracer for Solar Cells Qualification.

The temperature of the climate chamber was set at 70 °C to accelerate the degradation process. The value of the negative voltage potential was set at 1000 V. At specified time intervals, *I–V* characteristics were measured in darkness and under illumination. During the measurement, the constant temperature was maintained so as not to affect the measured *I–V* characteristics. In addition, the electroluminescence imaging was conducted.

The increasing thickness of the PSG layer also increases the PV cell reflection and, thus, negatively affects the electrical parameters such as short-circuit current I_{SC} [24]. The thickness of the PSG layer in the newly formed samples was set at 12 nm. This value has a minimal effect on PV cell parameters, as can be seen from the *I–V* characteristics (see Fig. 3) and the external quantum efficiency (see Fig. 4).

A standard layer of SiN_X silicon nitride (63 nm) was deposited for reference and newly formed samples. It should be noted that the parameters of the SiN_X layer have not been modified for newly created samples with the PSG layer. This is also evident from Fig. 5, where the sample with the PSG layer has a light blue surface.

The main parameters are summarized and compared in Table I. *I–V* characteristics are plotted in Fig. 3.

From the comparison, it is obvious that the PSG layer did not significantly affect PV cell parameters. Especially, the short-circuit current I_{SC} does not show a significant decrease in the sample with the PSG layer despite predicted reduction due to higher reflection [24].

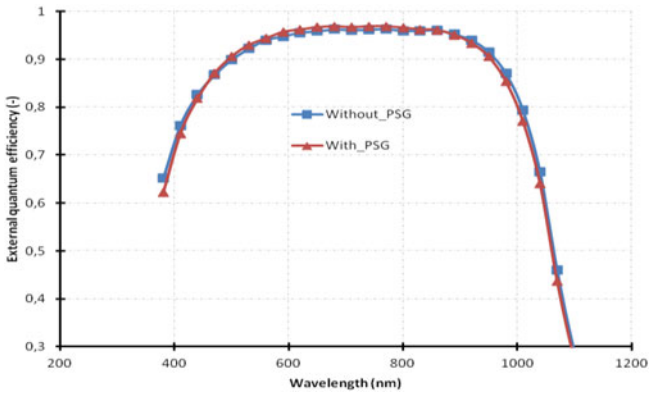

Fig. 4. External quantum efficiency of newly created (with PSG) and reference PV cells.

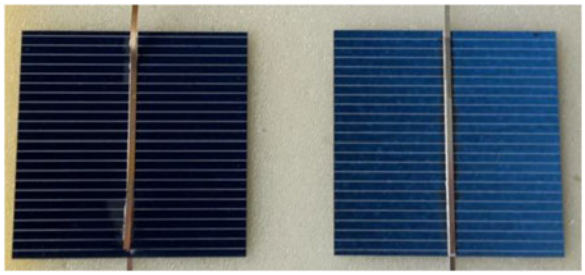

Fig. 5. PV cell samples. (Left) Reference sample. (Right) Sample with the PSG layer.

TABLE I
PARAMETERS OF THE REFERENCE SAMPLE (WITHOUT THE PSG LAYER) AND THE NEWLY CREATED SAMPLE (WITH THE PSG LAYER)

	I_{SC}(A)	V_{OC}(V)	I_{MAX}(A)	V_{MAX}(A)	P_{MAX}(W)	E_{FF} (%)
WithPSG	8.238	0.626	8.081	0.522	4.215	17.65
Without	8.233	0.625	8.084	0.525	4.244	17.74

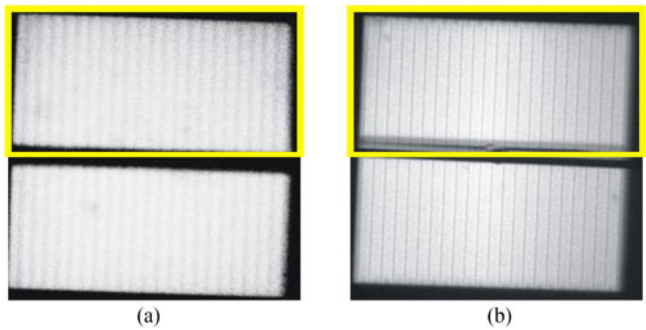

Fig. 6. Electroluminescence images of samples. (a) Reference sample. (b) New PSG layer. The yellow area shows the location of later-created PID cell degradation.

Fig. 4 illustrates the comparison of the external quantum efficiency of the samples with PSG and the reference cell without the PSG layer. It can be seen that the PSG sample values are similar to the measured values of the reference sample, even in the area of the blue color spectrum, where a decrease due to the increased reflection of the PSG layer would be expected. This finding confirms the results of the *I–V* characteristics, where the

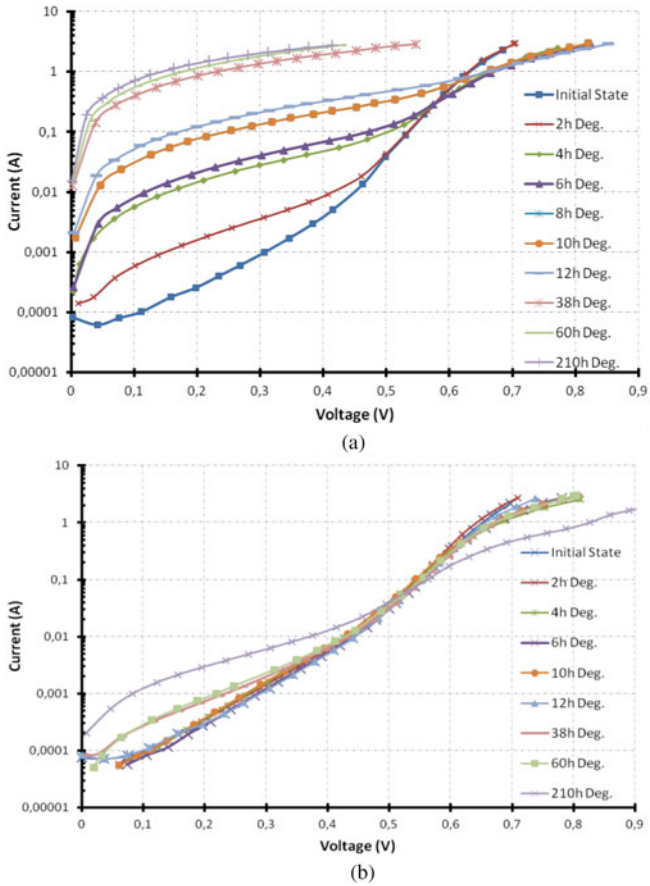

Fig. 7. *I–V* characteristics in the forward direction measured in the dark of (a) the reference sample and (b) the newly formed sample with the PSG layer.

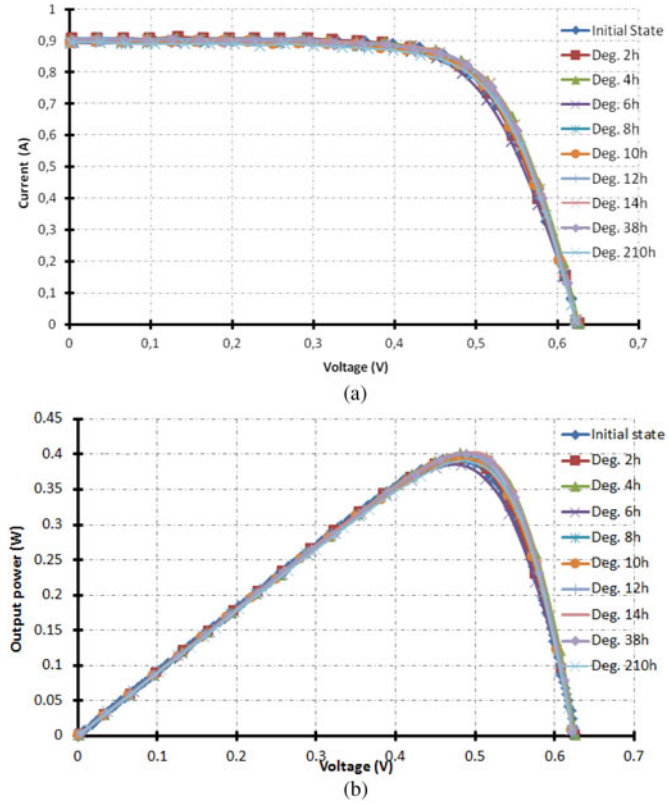

Fig. 8. (a) Current–voltage and (b) power characteristics of a newly formed sample of the PV cell with the PSG layer.

measured parameters of the samples are identical. From these results, it can be stated that the newly prepared structure with its electrical parameters does not differ from the reference sample.

III. Methods Used to Find the Level of Potential-Induced Degradation

For primary detection of PID, *I–V* measurement of dark characteristics was chosen using the *I–V* Curve Tracer for Solar Cells Qualification and the PASAN Sun Sim 3C flash tester for measurement under illumination. Measurements were done in an accredited laboratory, while maintaining the standard test conditions. *I–V* characteristics are accompanied with electroluminescence images taken by the G2CCD charge-coupled device (CCD) camera. For a more thorough inspection, the electron-beam-induced current (EBIC) analysis on the Tescan Vega 3 Xmu scanning electron microscope (SEM) with the LaB_6 cathode was done. Measurement of the external quantum efficiency was conducted on an apparatus using a trilattice monochromator and a halogen lamp.

IV. Results and Discussion

From the obtained electroluminescence image, it is evident that the surface of the initial PV cells before the PID is free from any defects—both of the reference sample (a) and the newly manufactured sample (b). The yellow section on both samples shows the area where PID occurred later (see Fig. 6).

Subsequent measurement of *I–V* characteristics in the dark was carried out at predetermined intervals (see Fig. 7). Before each measurement step, the samples were cooled to room temperature so that the temperature did not affect the measurement results.

I–V characteristics in the forward direction were plotted on the semilogarithmic scale. In such a representation, a change in the recombination region from 0 to 0.2 V can be seen, where a decrease in the shunt resistance R_{SH} is noticeable. From the measured values, there is a large decrease in the shunt resistance with the degradation time of the reference sample. A significant decrease in R_{SH} occurs after 4 h of degradation, where the exponential dependence changes to the ohmic. This change signifies the occurrence of p-n junction short circuits. The measured expression of degradation coincides with the measurement of PID degradation of the PV cells in [25]. The results of the newly created sample with the PSG layer show only a minimal increase in the current in the *I–V* characteristic recombination region, which clearly indicates the PID resistive properties of the newly created PV cell structure. A slight decrease in the shunt resistance occurs after 210 h of degradation. This decrease can be compared with the *I–V* characteristics measured under illumination exposure in Fig. 8, where performance characteristics do not show any noticeable drop in performance. The first two dependencies on Fig. 9 show the *I–V* characteristic and performance characteristics of the reference sample.

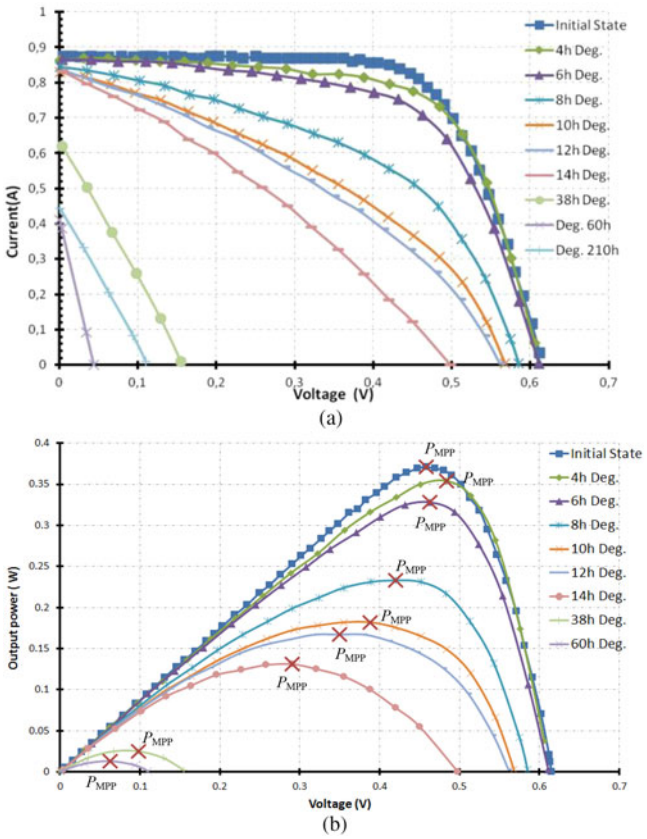

Fig. 9. (a) Current–voltage and (b) power characteristics after degradation time steps.

Dependencies in Fig. 9 show a high sensitivity of the reference sample to PID influence. Gradually increasing degradation time decreases the PV cell output power. The power output curve for the 210-h degradation time is not presented because of very low values. The most sensitive indicator of the PID is the PV cell shunt resistance (see Fig. 7), which is manifested after 4 h of degradation. It also correlates with *I–V* characteristics in the dark (see Fig. 7). However, with the increasing degradation time, the open-circuit voltage V_{OC} and the short-circuit current I_{SC} decrease. Decreasing of the shunt resistance R_{SH} also has a significant effect on the decrease of the fill factor [see Fig. 9(a)]. This is a typical effect of PID (see [26]). For a closer comparison of key PV cell parameters (I_{SC}, V_{OC}, R_{SH}, and P_{MAX}) depending on the degradation time, dependencies in Fig. 10 were created. Changes in the parameters of the new PV cell structure are minimal. From these results, it is possible to observe the PID resistive properties of the sample.

The comparison of the *I–V* characteristics of the newly created PV cells and reference structures is supplemented with electroluminescence images, which show the influence of the PID. Degraded PV cells contain short circuits in the p-n junction (see Fig. 11). Because of short circuits, charge carrier pairs cannot be generated due to current flow, as the CCD camera is not able to capture the electron–hole radiative recombination, and these areas are shown in black. On the surface of the reference cell, there is a gradual increase in local p-n junction short circuits, typical of the PID. On the other hand, in newly created PV cell structures, p-n junction short circuits were not observed.

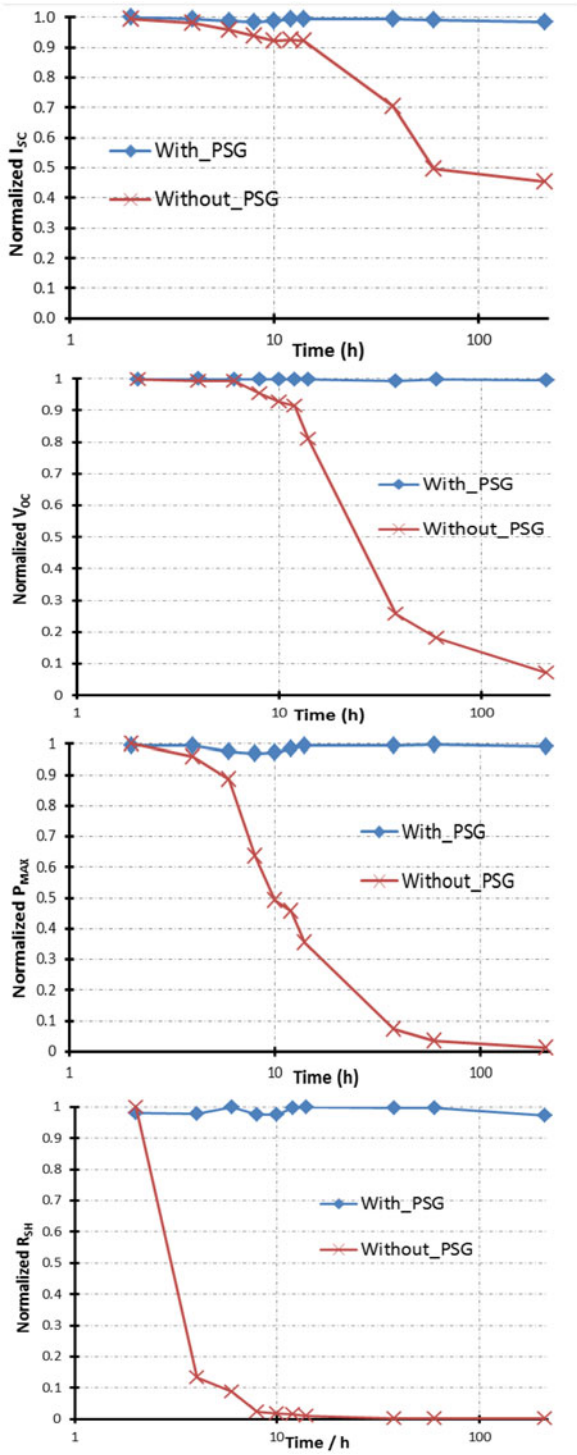

Fig. 10. Comparison of the main parameters of the reference and newly created PV cells depending on the time of the PID.

The degraded areas of the PV cell are bounded by a yellow box that indicates where the electric field was created by attaching the aluminum electrode.

In order to map the PID influence on key reference PV cell parameters, graphs were plotted in Fig. 10. It can be seen that the most sensitive parameter is the shunt resistance R_{SH}, which drops sharply after approximately 4 h of PID by about 90% of the default value. Another parameter that rapidly decreases in

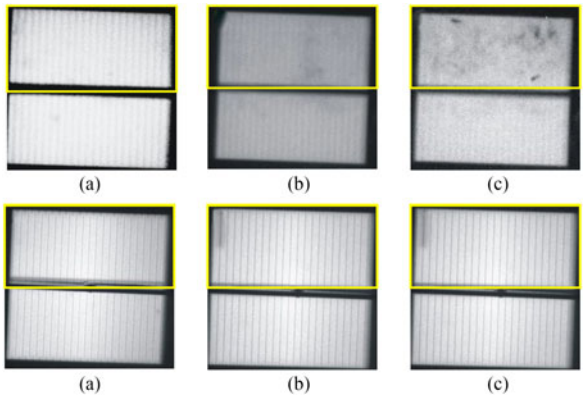

Fig. 11. Electroluminescence images of a reference and newly created sample of PV cells. (First row) Reference sample with observed PID in the form of short circuits. (Second row) Sample with the newly created structure. (a) Without degradation. (b) Fourteen hours of degradation. (c) Sixty hours of degradation.

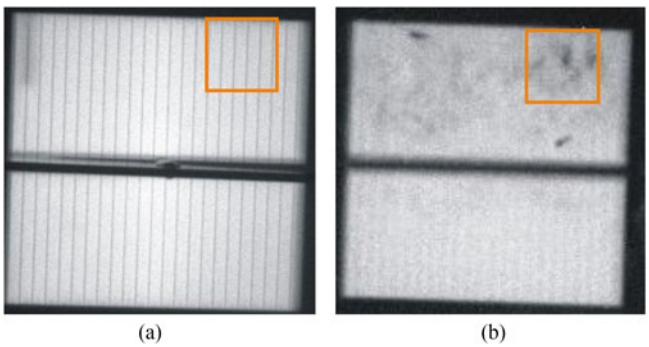

Fig. 12. Electroluminescence images of PV cells after 210 h of PID degradation. (a) Sample with the PSG layer. (b) Reference sample without the PSG layer.

value depending on the PID effect is the open-circuit voltage V_{OC}. This is associated with the decreasing shunt resistance and short circuits in the p-n junction. When comparing V_{OC} and I_{SC}, it is obvious that after 10 h of PID degradation, the values of V_{OC} decrease more steeply, which is due to PID-s character. It is further evident that a sample with the PSG layer has PID resistive properties for all plotted parameters.

The last high-resolution method that compares the reference and the newly created sample is the EBIC method of an electron scanning microscope, which is able to locate the p-n junction short circuits and compare them with the PV cell surface topography.

First, it was necessary to remove the PV cells from the laminated structure of the PV module using chemical decomposition of the polymerized EVA film. This process was followed by chemical cleaning of the surface and subsequent rinsing in deionized water.

EBIC images were taken on samples before degradation and after 210 h of degradation. The scanned area is marked in the orange frame on the electroluminescence images in Fig. 12. This area was selected in the PID part of the PV cell. Fig. 12(a) shows no short circuits after 210 h of PID. On the other hand, the influence of PID is noticeable in the sample without the PSG layer [see Fig. 12(b)].

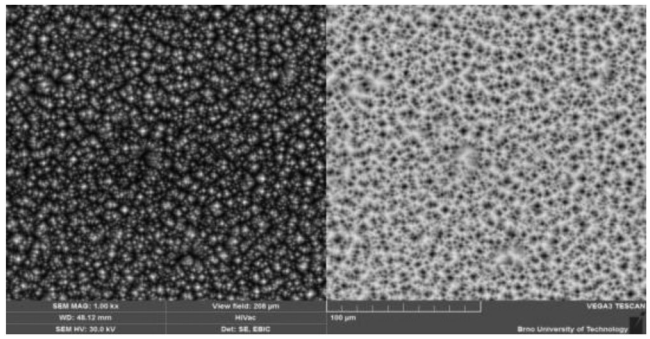

Fig. 13. SEM images of the newly created sample without localized short circuits after PID degradation. Magnification is 1000×.

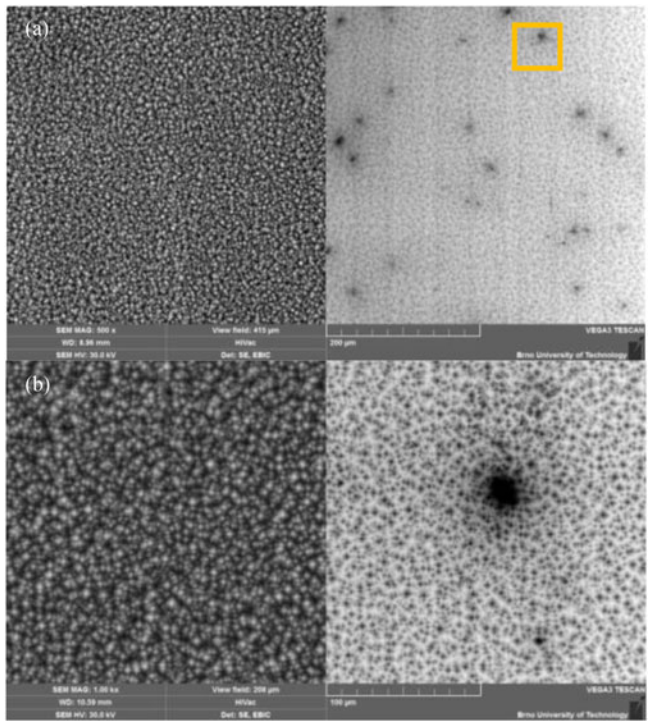

Fig. 14. SEM images of a reference cell with visible short circuits of p-n transition due to PID degradation. (a) Magnification is 500×. (b) Magnification is 1000×.

Fig. 13 shows the SEM images of the PV cell surface of the newly formed structure. On the left side of the Fig. 13 is a topography of the solar cell surface and on the right side is displayed the EBIC measurements of surface. The magnification of Fig. 13 is set at 1000 times. The pyramidal structure of the surface is evident. There is no defect in the surface topography, which confirms the results of the electroluminescence images that there are no short circuits due to PID in the sample.

In Fig. 14, the same analysis is performed for the reference PV cell sample. In the first picture [see Fig. 14(a)], the magnification is set at 500×. Surface topography on the left side of the image does not show any defects, while the EBIC analysis on the right side shows short circuits in p-n junctions (black areas). In Fig. 14(b), the orange rectangle indicates one of the localized short circuits with 1000× magnification.

As can be seen from Fig. 14(b), surface topography has shown no signs of defect at localized short circuit through the EBIC analysis, indicating a short circuit in the p-n junction. A zoomed dark point displayed by the accelerating voltage of 30 kV of the electron beam has a typical shape for the PID short circuits (see [4]).

V. Conclusion

In this research, p-type PV cells with the new structure resistive against PID were prepared. In the process of manufacturing the samples, the objective was to obtain a structure, which would not reduce the efficiency of the PV cells and other parameters such as the short-circuit current and the open-circuit voltage. This was achieved by the appropriate setting of the diffusion parameters for the preparation of the PSG layer. The PSG layer was left in the structure after the n-type emitter deposition. Samples with the PSG layer met the above-mentioned requirements. The values of the newly created samples correlated with the values of the reference samples, which confirmed the *I–V* characteristic measurements. This is also confirmed by the comparison of external quantum efficiency. The samples were further exposed to PID. Measuring results of dark and light *I–V* characteristics and an electron microscope analysis clearly show the PID resistive properties of the newly created samples.

These findings show that the PSG layer with a high phosphorus concentration has resistive properties against PID degradation. The PSG layer prevents sodium ions from penetrating into the silicon surface and, thus, prevents short circuit at the p-n junction. More specifically, due to phosphorus precipitates, the PSG layer has properties to keep sodium ions trapped in its volume.

On the other hand, it is necessary that the PSG layer does not affect the optical and electrical properties of the PV cell. The high thickness of the PSG layer increases the reflexivity of the surface, and the high concentration of electrically inactive phosphorus can increase the surface recombination velocity of the minor carriers. This can be prevented by a suitably adjusted diffusion process, especially in the first of two prediffusion steps. It is highly probable that PSG protection will also be applicable to other types of PV cells, such as passivated emitter and rear cells. This will be the subject of further scientific work.

Acknowledgment

The authors would like to gratefully acknowledge A. Poruba for helping with the consultation of the measured data.

References

[1] S. Pingel *et al.*, "Potential induced degradation of solar cells and panels," in *Proc. 35th IEEE Photovoltaic Spec. Conf.*, 2010, pp. 2817–2822.

[2] J. Bauer *et al.*, "On the mechanism of potential-induced degradation in crystalline silicon solar cells," *Phys. Status Solidi—Rapid Res. Lett.*, vol. 6, no. 8, pp. 331–333, 2012.

[3] V. Naumann, C. Hagendorf, S. Grosser, M. Werner, and J. Bagdahn, "Micro structural root cause analysis of potential induced degradation in c-Si solar cells," *Energy Procedia*, vol. 27, pp. 1–6, 2012.

[4] V. Naumann *et al.*, "Microstructural analysis of crystal defects leading to potential-induced degradation (PID) of Si solar cells," *Energy Procedia*, vol. 33, pp. 76–83, 2013.

[5] V. Naumann *et al.*, "Explanation of potential-induced degradation of the shunting type by Na decoration of stacking faults in Si solar cells," *Sol. Energy Mater. Sol. Cells*, vol. 120, pp. 383–389, 2014.

[6] V. Naumann, D. Lausch, A. Hähnel, O. Breitenstein, and C. Hagendorf, "Nanoscopic studies of 2D-extended defects in silicon that cause shunting of Si-solar cells," *Phys. Status Solidi*, vol. 12, no. 8, pp. 1103–1107, 2015.

[7] V. Naumann, C. Brzuska, M. Werner, S. Großer, and C. Hagendorf, "Investigations on the formation of stacking fault-like PID-shunts," *Energy Procedia*, vol. 92, pp. 569–575, 2016.

[8] D. Lausch *et al.*, "Sodium outdiffusion from stacking faults as root cause for the recovery process of potential-induced degradation (PID)," *Energy Procedia*, vol. 55, pp. 486–493, 2014.

[9] V. Naumann *et al.*, "The role of stacking faults for the formation of shunts during potential-induced degradation of crystalline Si solar cells," *Phys. Status Solidi—Rapid Res. Lett.*, vol. 7, no. 5, pp. 315–318, 2013.

[10] K. Hara, S. Jonai, and A. Masuda, "Potential-induced degradation in photovoltaic modules based on n-type single crystalline Si solar cells," *Sol. Energy Mater. Sol. Cells*, vol. 140, pp. 361–365, 2015.

[11] V. Naumann *et al.*, "Potential-induced degradation at interdigitated back contact solar cells," *Energy Procedia*, vol. 55, pp. 498–503, 2014.

[12] R. Swanson *et al.*, "The surface polarization effect in high-efficiency silicon solar cells." in *Proc. 15th Int. Photovolt. Sci. Eng. Conf.*, 2005, p. 4.

[13] S. Yamaguchi, A. Masuda, and K. Ohdaira, "Potential-induced degradation behavior of n-type single-crystalline silicon photovoltaic modules with a rear-side emitter," in *Proc. IEEE 43rd Photovoltaic Spec. Conf.*, 2016, pp. 938–942.

[14] J. Oh, S. Bowden, and G. S. TamizhMani, "Potential-induced degradation (PID): Incomplete recovery of shunt resistance and quantum efficiency losses," *IEEE J. Photovolt.*, vol. 5, no. 6, pp. 1540–1548, Nov. 2015.

[15] J. Kapur, K. M. Stika, C. S. Westphal, J. L. Norwood, and B. Hamzavytehrany, "Prevention of potential-induced degradation with thin ionomer film," *IEEE J. Photovolt.*, vol. 5, no. 1, pp. 219–223, Jan. 2015.

[16] M. Barbato *et al.*, "Potential induced degradation of N-type bifacial silicon solar cells: An investigation based on electrical and optical measurements," *Sol. Energy Mater. Sol. Cells*, vol. 168, pp. 51–61, 2017.

[17] M. Koehl and S. Hoffmann, "Impact of rain and soiling on potential induced degradation," *Prog. Photovolt.: Res. Appl.*, vol. 24, no. 10, pp. 1304–1309, 2016.

[18] S. Hoffmann and M. Koehl, "Effect of humidity and temperature on the potential-induced degradation," *Prog. Photovolt.: Res. Appl.*, vol. 22, no. 2, pp. 173–179, 2014.

[19] J. Hylsky, D. Strachala, and J. Vanek, "Temperature influence on the PID affected photovoltaic modules regeneration," *ECS Trans.*, vol. 74, no. 1, pp. 277–283, Dec. 2016.

[20] S. Koch *et al.*, "Potential Induced degradation effects on crystalline silicon cells with various antireflective coatings," in *Proc. 27th Eur. Photovoltaic Sol. Energy Conf. Exhib.: Silicon Sol. Cell Improvements*, 2012, pp. 1985–1990.

[21] J. Oh *et al.*, "Further studies on the effect of SiN_x refractive index and emitter sheet resistance on potential-induced degradation," *IEEE J. Photovolt.*, vol. 7, no. 2, pp. 437–443, Mar. 2017.

[22] P. Negrini, D. Nobili, and S. Solmi, "Kinetics of phosphorus predeposition in silicon using $POCl_3$," *J. Electrochem. Soc.*, vol. 122, no. 9, pp. 1254–1260, 1975.

[23] A. Dastgheib-Shirazi *et al.*, "Relationships between diffusion parameters and phosphorus precipitation during the $POCl_3$ diffusion process," *Energy Procedia*, vol. 38, pp. 254–262, 2013.

[24] C.-H. Du *et al.*, "A well-controlled PSG layer on silicon solar cells against potential induced degradation," *ECS J. Solid State Sci. Technol.*, vol. 4, no. 3, pp. P97–P100, Dec. 2014.

[25] S. Yamaguchi and K. Ohdaira, "Degradation behavior of crystalline silicon solar cells in a cell-level potential-induced degradation test," *Sol. Energy*, vol. 155, pp. 739–744, 2017.

[26] A. Masuda *et al.*, "Microscopic aspects of potential-induced degradation phenomena and their recovery processes for p-type crystalline Si photovoltaic modules," *Current Appl. Phys.*, vol. 16, no. 12, pp. 1659–1665, 2016.

Authors' photographs and biographies not available at the time of publication.